International Journal of Nanomedicine

Dovepress

open access to scientific and medical research

Open Access Full Text Article

ORIGINAL RESEARCH

Lactobacillus-Polydopamine System for Targeted Drug Delivery in Overactive Bladder: Evidence from Bladder Cell Spheroids, Rat Models, and Urinary Microbiome Profiling

Xiaolong Wang[1,2,*], Guanyi Wang[2,*], Peibin Cen[1,*], Hongyu Lan[1], Linfa Guo[2], Zuhaer Yisha[2], Aodun Gu[2], Guiyong Liu[3], Zijian Wang[2], Tongzu Liu[2,4–8], Qingfeng Yu[1,9–11]

[1]Department of Urology, The First Affiliated Hospital of Guangzhou Medical University, Guangzhou, People's Republic of China; [2]Department of Urology, Zhongnan Hospital of Wuhan University, Wuhan, People's Republic of China; [3]Department of Urology, Qianjiang Central Hospital of Hubei Province, Qianjiang, People's Republic of China; [4]Hubei Key Laboratory of Urological Diseases, Wuhan University, Wuhan, People's Republic of China; [5]Hubei Clinical Research Center for Laparoscopic/Endoscopic Urologic Surgery, Zhongnan Hospital of Wuhan University, Wuhan, People's Republic of China; [6]Institute of Urology, Wuhan University, Wuhan, People's Republic of China; [7]Hubei Medical Quality Control Center for Laparoscopic/Endoscopic Urologic Surgery, Zhongnan Hospital of Wuhan University, Wuhan, People's Republic of China; [8]Wuhan Clinical Research Center for Urogenital Tumors, Zhongnan Hospital of Wuhan University, Wuhan, People's Republic of China; [9]Guangdong Provincial Key Laboratory of Urological Diseases, Guangzhou Medical University, Guangzhou, People's Republic of China; [10]Guangdong Engineering Research Center of Urinary Minimally Invasive Surgery Robot and Intelligent Equipment, Guangzhou Medical University, Guangzhou, People's Republic of China; [11]Guangzhou Institute of Urology, Guangzhou Medical University, Guangzhou, People's Republic of China

*These authors contributed equally to this work

Correspondence: Tongzu Liu, Department of Urology, Zhongnan Hospital of Wuhan University, Wuhan, People's Republic of China, Email liutongzu@163.com; Qingfeng Yu, Department of Urology, The First Affiliated Hospital of Guangzhou Medical University, Guangzhou, People's Republic of China, Email sunriseyu@yeah.net

Introduction: Overactive bladder (OAB) is a highly prevalent condition with limited treatment options due to poor efficacy, side effects, and patient compliance. Novel drug delivery systems that can target the bladder wall may improve OAB therapy.

Methods: We explored a polydopamine (PDA)-coated lactobacillus platform as a potential carrier for localized OAB treatment. Urinary microbiome profiling was performed to identify the presence of lactobacillus in healthy and OAB groups. Lactobacillus-PDA nanoparticles were synthesized and characterized by electron microscopy and spectrophotometry. A rat bladder perfusion model and human bladder smooth muscle cell spheroids were used to assess the distribution and penetration of the nanoparticles. The efficacy of the Lactobacillus-PDA system (LPS) for delivering the antimuscarinic drug solifenacin was evaluated in an OAB rat model.

Results: Urinary microbiome profiling revealed lactobacillus as a dominant genus in both healthy and OAB groups. The synthesized Lactobacillus-PDA nanoparticles exhibited uniform size and optical properties. In the rat bladder perfusion model, the nanoparticles distributed throughout the bladder wall and smooth muscle without toxicity. The nanoparticles also penetrated human bladder smooth muscle cell spheroids. In the OAB rat model, LPS facilitated the delivery of solifenacin and improved treatment efficacy.

Discussion: The results highlight LPS as a promising drug carrier for targeted OAB therapy via penetration into bladder tissues. This bacteriotherapy approach may overcome limitations of current systemic OAB medications. Lactobacillus, a probiotic bacterium present in the urinary tract microbiome, was hypothesized to adhere to and penetrate the bladder wall when coated with PDA nanoparticles, making it a suitable candidate for localized drug delivery.

Keywords: polydopamine, lactobacillus, nano material, drug delivery, overactive bladder

Introduction

Overactive bladder (OAB) is a highly prevalent condition characterized by urinary urgency that reduces quality of life, which is still the leading cause of lower urinary tract symptoms (LUTS).[1] OAB and LUTS pose a considerable health

Received: 5 April 2024
Accepted: 17 July 2024
Published: 15 August 2024

Graphical Abstract

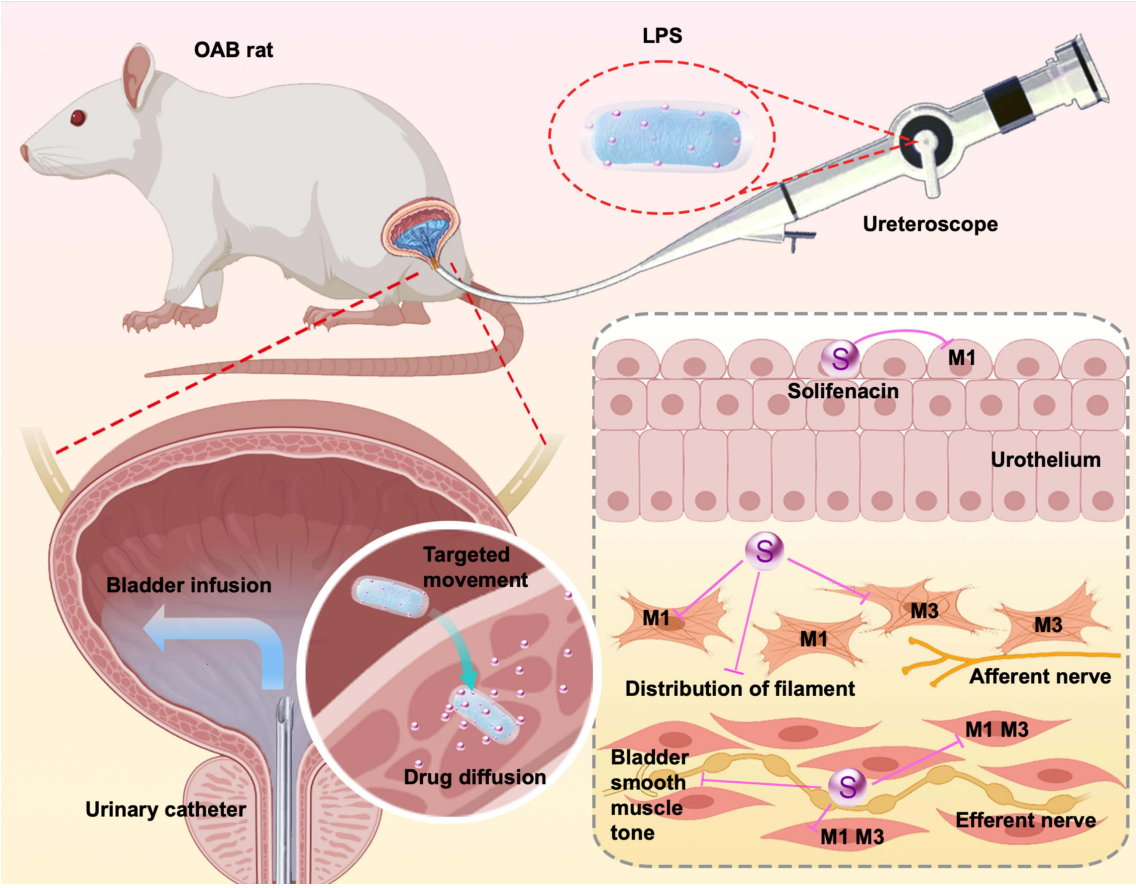

challenge, particularly among the elderly female population in the United States, European, Asia, and other countries.[2–4] An exploration into the epidemiological evidence surrounding OAB-associated LUTS reveals a significant impact on the well-being of aging women. Delving into the pathology and mechanisms underlying LUTS is crucial for developing more effective medications and therapeutic strategies, holding substantial implications for public health and economy.[5] Globally, LUTS were highly prevalent, affecting an estimated 2.3 billion people in 2018, with men constituting 44.7% of those affected.[6] Men experiencing LUTS contend not only with bothersome symptoms like nocturia and urgency but also face adverse psychological consequences such as anxiety and depression, further contributing to a substantial financial burden.[7] Understanding and addressing the complexities of OAB-associated LUTS are imperative for improving the overall health and quality of life of affected individuals worldwide, encompassing both male and female patient populations.

OAB pathophysiology centers on abnormal bladder smooth muscle tone during filling, with inappropriate contractions when relaxation should occur. This dysfunction underpins OAB diagnosis and treatment monitoring, combining objective urodynamic measurements with subjective patient reports. Understanding these muscular mechanisms is key to effective OAB management.[8] Despite a higher prevalence of OAB in developed regions, current therapeutic interventions remain limited. Notably, first-line antimuscarinic medications are insufficiently effective for over 50% of patients, underscoring a substantial unmet treatment need. This inadequacy is further exacerbated by limitations in drug delivery that impede medications such as solifenacin, which is a bladder-selective muscarinic receptor (M-receptor) antagonist, and other antimuscarinic agents.[9] The low concentration of these drugs attained in bladder tissue attenuates their efficacy, while higher concentrations confer risks of toxicity and adverse effects on non-target organ systems.[10] Consequently,

there is an exigent need to develop a targeted drug delivery system to surmount these challenges, representing a pivotal advancement in OAB management.

Our current understanding of the pathophysiology of LUTS has relied on the long-held dogma that the bladder is sterile.[11] However, this dogma has been challenged by numerous reports describing the existence of resident bacterial communities in urine obtained from bladders of asymptomatic men and women without clinical urinary tract infection.[12] The National Institutes of Health (NIH) funded Human Microbiome Project (HMP) represent large-scale interdisciplinary efforts to profile the human microbiome across body sites including the GI tract, mouth, vagina, skin, nasal cavity, and skin. The bladder was initially excluded from testing in the HMP, as the prevailing dogma upheld that it was a sterile environment, coupled with intricacies in procuring representative samples.[13] However, over the past few years, our team and other researchers have demonstrated that a resident microbial community inhabits the bladder, termed the urinary microbiome.[14] In healthy states, the bladder microbiota predominantly exerts beneficial bioactivity rather than promoting pathogenesis.[15] Lactobacillus, Gardnerella, and Streptococcus are among the most prevalent genera found in the bladder microbiota of healthy women.[16–18] Research has shown that healthy male bladders tend to contain more Enterococcus, Proteus, and Klebsiella.[19,20] Evidence shows Lactobacillus may be a benign microbe in the human urinary system. A decline in Lactobacillus abundance has been linked to clinical disorders, as Lactobacillus insufficiency promotes colonization by disease-causing uropathogens.[21] In this study, 16S rRNA gene sequencing of bladder tissue rather than urine samples was utilized to examine the microbial composition and functional connections of the urinary microbiome. Our analyses identified Lactobacillus as one of the predominant genera inhabiting the bladder microbiota, underscoring its prospective role as a live biotherapeutic for alleviating lower urinary tract symptoms.

In contemporary nanomedicine research for bladder disease treatment, the use of nanomaterials such as Polydopamine-based nanomaterials (PDA) and other material-based drug delivery systems has garnered considerable attention.[22] However, a major challenge in this field is the limited bladder retention and smooth muscle cell targeting of nanomaterials. To address this constraint, microbe-coating of nanomaterials has emerged as a promising strategy.[23] This innovative approach involves the immobilization of benign microbes onto a drug nanocarrier to enhance overall delivery efficacy.[24,25] Two critical facets underpin the potential of this methodology: first, the ability of microbes to embed themselves within bladder tissue and stay in place for prolonged durations, thereby mitigating the issue of inadequate retention; second, the microbes serve as biocompatible carriers, enabling localized and concentrated co-delivery of nanomaterials and therapeutic agents.

This integration of microbial vectors with nanocarriers holds tremendous promise in surpassing current limitations associated with bladder disease treatment, proffering a novel conduit for optimized drug delivery and therapeutic impact. In this work, we developed a Lactobacillus-PDA system (LPS) incorporating recent advances in nanomaterial research. Polydopamine nanoparticles adsorb antimuscarinic medications via π-π stacking and charge interactions. Lactobacillus adhesion to bladder tissue retains LPS and targeted to smooth muscle, increasing local drug concentrations.

LPS demonstrates minimal toxicity in cellular and rodent models. The Lactobacillus coating enhances biocompatibility and sustained drug release by reducing nanoparticle aggregation. Our findings indicate that LPS represents a novel bacteria-based nanomaterial carrier for targeted OAB therapy. We aimed to develop a microbial vector-nanocarrier system to deliver a therapeutic reagent that can feasibly penetrate the bladder wall and remain in the bladder smooth muscle to continually inhibit muscarinic receptors. Integrating the utilization of microbial function and nanomaterial design attempts to achieve a balance between drug delivery and biocompatibility. Consequently, we successfully created a well-engineered LPS system with hierarchical structures and bioinstructive materials that promote long-term patency and remodelling of bladder smooth muscle for OAB treatment. In this study, solifenacin-loaded LPS enhances treatment efficacy in 3D bladder spheroid and rat models by synergizing targeted nanodelivery with native bladder microbiota. In summary, engineered bacteria-derived nanomaterials constitute a promising therapeutic platform for improved OAB management via localized pharmacologic delivery.

Material and Methods

Cell and Reagents

Human bladder smooth muscle cells (hBSMCs) were utilized as an in vitro model to evaluate the effects of PLS and solifenacin on cell viability and contractility. PDA hydrochloride and polyetherimide (PEI, Mw = 10,000 Da) were

purchased from Xian Ruixi Biological Technology Co. Ltd, China. Solifenacin (YM905 free base), which were purchased from MedChemExpress (MedChemExpress LLC, Monmouth Junction, NJ, USA), is a novel muscarinic acetylcholine receptor antagonist with reported pKi values of 7.6, 6.9, and 8.0 at the M1, M2, and M3 receptor subtypes, respectively.[26] Peak plasma levels are reached 3–8 hours following oral administration. Solifenacin has 98% plasma protein binding and is highly distributed to peripheral tissues. Solifenacin has 90% bioavailability and a long half-life of 45–68 hours. Lactobacillus is a genus of gram-positive, facultative anaerobic or microaerophilic, rod-shaped bacteria that are a major part of the lactic acid bacteria group. The culture medium used for growth of Lactobacillus (Medium Label CM 0006, Tianshengxing Biological Technology Co., Ltd., Wuhan, China) contains casein peptone, beef extract, yeast extract, glucose, sodium acetate, ammonium citrate, Tween 80, K2HPO4, MgSO4·7H2O, MnSO4·H2O, CaCO3, agar, and distilled water at pH 6.8. Lactobacillus are fastidious bacteria with specific nutritional requirements, including amino acids, peptides, and carbohydrate energy sources. The medium provides these growth factors along with salts, buffering agents, and surfactants to maintain suitable pH, osmotic, and oxygen transfer conditions for aerobic growth at 37°C. The effects of these pharmacological agents on hBSMCs viability and contractility were subsequently evaluated.

Human Tissue

Human bladder trigone tissue specimens were procured with informed consent from 20 patients undergoing transurethral resection of bladder tumors at Zhongnan Hospital, Wuhan University in accordance with ethical guidelines outlined in the Declaration of Helsinki. The Wuhan University Institutional Review Board reviewed and approved the study protocol before its initiation. All experimental procedures were conducted in accordance with the guidelines and regulations set forth by the Medical Ethics Committee of Zhongnan Hospital, Wuhan University. The research received ethical approval under Scientific Ethical Approval No. 2019108 and No. 2024093. During the resection surgery, trigone tissue samples were surgically excised from all 20 patients and promptly immersed in pre-cold organ preservation solution. A qualified pathologist conducted gross and histological examinations of all procured tissue samples. Microbial DNA extraction was attempted on all 20 specimens. Sufficient microbial DNA for further analysis was successfully isolated from 6 of the 20 trigone tissue samples using a commercially available kit according to the manufacturer's instructions.

Bacterial 16S rRNA Analysis

Microbial DNA was isolated from 6 qualified human bladder trigone tissue samples. The V4 region of the bacterial 16S rRNA gene was PCR amplified using primers 515F and 806R. PCR products were purified with AMPure XP beads. Indexed sequencing adapters were attached using the Nextera XT kit. The 16S libraries were quantified, pooled, and sequenced on the PacBio RS II platform (Biomarker Technologies, Beijing, China) to analyse microbial abundance and diversity. Raw PacBio circular consensus sequencing reads were processed through the DADA2 pipeline in QIIME2 for quality control, dereplication, chimera removal, and inference of amplicon sequence variants (ASVs). ASVs were taxonomically classified against the SILVA database using q2-feature-classifier. Alpha and beta diversity metrics were calculated in QIIME2. Differential abundance testing was performed in R using DESeq2.

Preparation of Lactobacillus-Polydopamine Composites and Solifenacin Loading

Lactobacillus species (Tianshengxing Biological Technology Co., Ltd., Wuhan, China), were anaerobically cultured in deMan, Rogosa and Sharpe (MRS) broth and harvested in stationary growth phase. Lactobacillus were washed in phosphate-buffered saline (PBS) and resuspended to a concentration of 109 colony-forming units per milliliter (CFU/mL).[27] Lactobacillus were cultured overnight, centrifuged at 3000 rpm for 5 min, and the supernatant was removed, and the pellet was washed 1–3 times. Lactobacillus density was adjusted to an OD 600 of approximately 0.5, then diluted 5-fold. 10, 5, 2, 1, and 0.5 mL of diluted Lactobacillus suspension were aliquoted into separate 50 mL centrifuge tubes and centrifuged to remove the supernatant. PDA solution (0.1, 0.5, 2 mg/mL PDA nanoparticles) was prepared and the pH was adjusted to 8.5 with ammonium hydroxide. A 10 mL aliquot of PDA solution was added to each tube, thoroughly mixed, and allowed to react overnight on a shaker at 37°C. The tubes were then centrifuged, and the resulting products were collected. This procedure effectively coated Lactobacillus with a PDA layer for subsequent experimentation.

For solifenacin delivery, we employed a concentration of 500 nM, as established through our preliminary studies.[28] The drug was co-incubated with PDA-coated Lactobacillus for 24 hours at 37°C, facilitating the incorporation of solifenacin molecules into the PDA layer. Prior to use, the mixture was sonicated for 30 seconds using an ultrasonic disperser (Scientz-1500F, NINGBO XINZHI, Zhejiang Province, China; frequency: 20 kHz; power: 100 W; dispersion head: 18 mm; dispersion volume: 50 mL). This approach allowed for the orientation of solifenacin by Lactobacillus, enabling targeted delivery to the bladder smooth muscle layer (Figure 1. Fabrication process).

Transmission Electron Microscopy Imaging and Sample Viability

Transmission electron microscopy (TEM) (Hitachi High-Tech Co., Ltd, Hitachi, Japan) was employed to visually inspect the Lactobacillus-polydopamine (PDA) solution and confirm immobilization of Lactobacillus decorated with PDA nanoparticles onto the gold TEM grid surface. Briefly, 5 µL of sample was deposited onto a 300 mesh formvar/carbon coated gold TEM grid and allowed to adhere for 5 minutes. Excess sample was wicked away and grids were washed in distilled water prior to staining with 1% aqueous uranyl acetate for 1 minute. Grids were imaged using a Hitachi TEM system operated at 80 kV. Multiple random views were acquired across each grid. To assess sample viability following grid preparation, LIVE/DEAD BacLight viability and counting assay was conducted by depositing stained bacteria on a hemocytometer and imaging on a HITACHI Ti2 fluorescent microscope (Hitachi High Technologies America, Inc., Tokyo, Japan). As the TEM grid preparation requires multiple saline washes, no significant compromise in bacterial cell viability was observed relative to the original sample.

TEM was utilized to obtain images of PDA nanoparticles synthesized at varying concentrations. The nanoparticle diameters were measured by digital image analysis using ImageJ software. A total of 20 nanoparticles were measured per sample. The distribution of nanoparticle sizes for each PDA concentration was further analyzed using OriginPro 21 software (OriginLab Northampton, Massachusetts, USA). Frequency plots visually representing the size distributions are included.

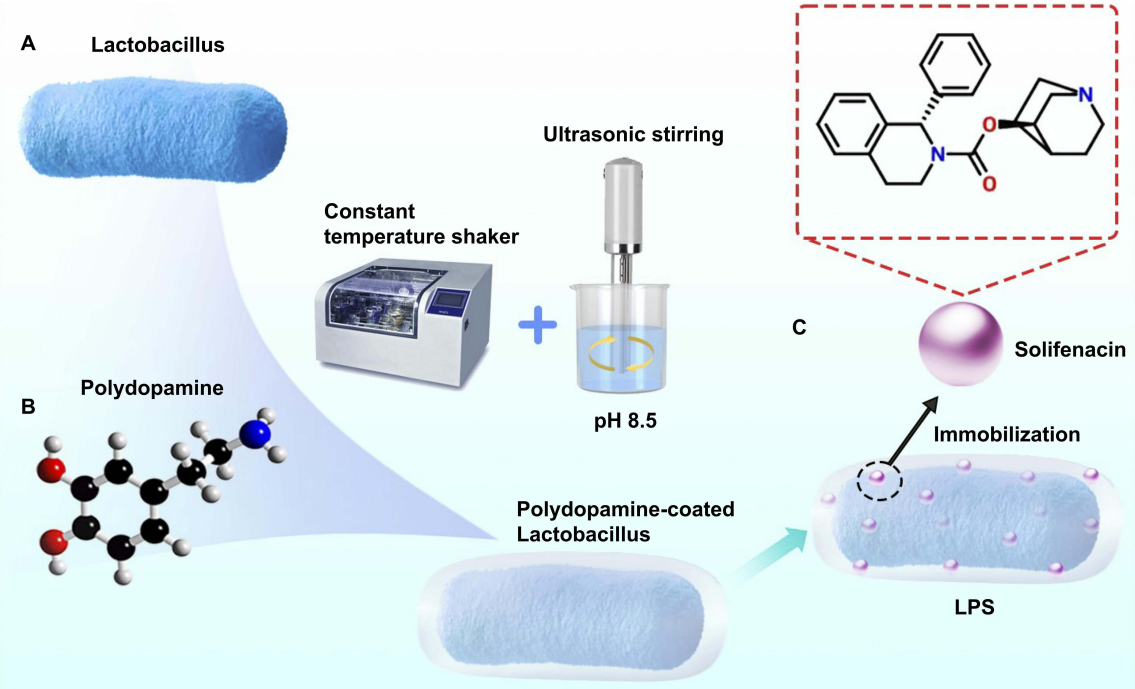

Figure 1 Fabrication process of LPS. (**A**) PDA was covalently conjugated to Lactobacillus surfaces, creating a microbe-assisted drug delivery system LPS. (**B**) PDA solution (10 mL) was incubated with Lactobacillus overnight at 37°C in a constant temperature shaker, followed by centrifugation and product collection. (**C**) Solifenacin (500 nM) was incorporated into the PDA layer via 24-hour co-incubation at 37°C, exploiting π-π stacking and hydrophobic interactions. The mixture was briefly sonicated (30 s, 20 kHz, 100 W) prior to use via a ultrasonic stirring machine. This approach enabled sustained solifenacin release from viable LPS.

Lactobacillus Gram Staining in Rat Bladder

Male Sprague-Dawley rats were subjected to partial bladder outlet obstruction surgery, followed by transurethral instillation of the Lactobacillus-PDA complexes or PBS control directly into the bladder lumen. At 2 hours post-treatment, bladders were excised and prepared for microscopic analysis. Rat bladders were extracted and immediately fixed in 4% paraformaldehyde for 24 hours. The tissues were then cryoprotected through a sucrose gradient (10%, 20%, 30% sucrose in PBS), embedded in optimal cutting temperature compound, and cryosectioned at 10 μm thickness. Tissue sections were adhered to charged glass slides. For staining, slides were air dried for 30 minutes before heat fixing. Crystal violet was applied for 1 minute, followed by washing with water. Iodine solution was then applied for 1 minute followed by decolorization with 95% ethanol. The decolorizer was washed off with water. Safranin counterstain was applied for 45 seconds before a final wash in water. Slides were allowed to fully air dry. This Gram stain procedure results in a purple-stained cell wall and blue cytoplasm in Gram-positive bacteria, while Gram-negative bacteria stain pink-red. Images were taken under a brightfield microscope to identify the presence of Gram-positive Lactobacillus (purple) within the bladder tissue (red). Quantification of Lactobacillus within regions of interest in the bladder was performed using ImageJ software.

Bladder Cell Spheroids Formation

Human bladder smooth muscle cell spheroids were generated to evaluate the effects of a LPS drug delivery system as a potential urological therapy. Spheroids were formed by seeding 2×10^4 human bladder smooth muscle cells per well into ultra-low attachment plates (LV-ULA002-6W, LV BioTech, Shenzhen City, China) coated with Matrigel (1:100 dilution) (Corning Matrigel matrix, Corning®, New York City, USA). The plates were maintained under continuous low-speed orbital agitation at 37°C/5% CO2 for 72 hours to allow spheroid self-assembly. Spheroid formation and diameter were monitored by phase contrast microscopy and quantified using image analysis software. To assess therapeutic effects, spheroids were treated with polydopamine-coated Lactobacillus delivering 500 nM of the drug solifenacin for 24 hours prior to fixation in paraformaldehyde.

OAB Rat Model Validation

An animal model of bladder outlet obstruction (BOO) was induced to mimic OAB in 25 male Sprague-Dawley rats weighing 250–280 g obtained from the Guangdong Medical Laboratory Animal Center, Guangzhou, China.[29] All animal experiments were carried out in accordance with protocols approved by the Institutional Animal Care and Use Committee of the Guangzhou Medical University, Guangzhou, China. After a 7-day acclimatization period, the rats were randomly allocated to either the BOO surgery group (n=20) or the control group (n=5). Under isoflurane anesthesia, a lower midline abdominal incision was made to expose the proximal urethra. In the BOO group, a 1 mm diameter needle was placed parallel to the urethra and a 4–0 silk suture (Ethicon, Johnson & Johnson MedTech, NJ, USA) was tied around the urethra. The needle was then removed, leaving the ligature in place. Gentle compression of the bladder was performed to ensure appropriate tightness of the ligature without complete obstruction. The abdominal incision was then closed.

To verify the successful induction of OAB, urination frequency was assessed in the BOO and sham groups at 2 weeks post-surgery using Copper monosulfide (CuS) filter paper method. The rats were individually housed in metabolic cages with filter paper placed underneath to absorb all voided urine. Urination frequency was calculated by counting the number of urine spots on the filter paper over a 1 hour period. Rats the BOO group demonstrated a significant increase in urination frequency compared to sham group, indicating successful induction of OAB.

OAB Rat Model Treatment with LPS

Male Sprague-Dawley rats underwent partial urethral obstruction surgery to induce overactive bladder (n=20 total). Two weeks post-induction, rats were divided into four groups (n=5 each) for intravesical treatment: blank control, sham control, 500 μM solifenacin suspension, and Lactobacillus-polydopamine nanoparticles loaded with 500 μM solifenacin (LPS-treated). Treatments were instilled into the emptied bladder through a catheter and retained for 2 hours by urethral

occlusion. Bladders were then excised and processed for hematoxylin/eosin staining (H-E staining), Masson staining, and immunofluorescence labeling of smooth muscle actin (SMA) and filament proteins.

H-E Staining and Masson Staining

The potential effects of LPS on cell spheroid structure were investigated using H-E and Masson staining on sections from control and LPS-treated (500 nM, 24 h) groups. Stained sections were analyzed by ImageJ to quantify smooth muscle remodelling and fibrosis level. Specifically, the area fraction of collagen fibers and number of inflammatory cells were measured in each spheroid section. Statistical comparisons of these histological parameters were performed between the control and LPS-treated groups. This quantitative image analysis enabled standardized comparisons of smooth muscle extracellular matrix composition and inflammation resulting from LPS treatment in the 3D spheroid model.

Immunofluorescence Staining

Immunofluorescence (IF) staining was performed on cell spheroids from three experimental groups: untreated control, solifenacin-treated, and LPS-treated. For bladder tissue analysis in the overactive bladder (OAB) rat model, rats were divided into four groups (n=5 per group): 1) non-treated control, 2) sham, 3) solifenacin-treated, and 4) LPS-treated. To perform IF staining, we utilized an antibody-based method that allowed for the detection and localization of specific antigens within various tissue types or cell preparations. An indirect IF staining method was used, which involved a primary antibody binding to the target antigen and a secondary antibody carrying a fluorophore that bound to the primary antibody. After the cell spheroids were fixed with 4% paraformaldehyde and permeabilized with 0.1% Triton X-100, 5% bovine serum albumin (BSA) was incubated with the samples to block nonspecific binding. Primary antibodies against smooth muscle biomarkers, such as bladder smooth muscle actin (anti α-SMA, 1:1000) (Huabio, Hangzhou City, China) and bladder myo-filaments (anti Filamin A, 1:500) (Huabio, Hangzhou City, China), were applied to the samples, which were incubated overnight at 4 °C. We washed the samples via phosphate-buffered saline (PBS) and subsequently applied secondary antibodies conjugated with Alexa Fluor 488 or 594, followed by incubation for one hour at room temperature. After counterstaining the samples with 4',6-diamidino-2-phenylindole (DAPI), which specifically labels nuclei, we mounted them on glass slides and acquired confocal images via a Leica TCS SP8 microscope. Finally, we utilized ImageJ software to analyze the images and quantify the fluorescence intensity of primarily SMA and filament.

Data Analysis

To analyze microbe distribution and potential functional gene expression, 16S rRNA sequencing was utilized to profile the microbiome of human trigone tissue, as well as a OAB rat model that was previously developed in our lab and treated with solifenacin. Various analytical pipelines were employed to identify the effects of solifenacin treatment on smooth muscle cells. Bladder cell spheroid proliferation was examined through H-E, Masson's trichrome, and immunofluorescence staining techniques. One-way ANOVA with multiple comparisons testing was used to determine statistical significance of differences in staining levels between conditions. Additionally, bladder wall thickness, bladder luminal area, and area of DAPI/α-SMA/filament staining were compared between groups using one-way ANOVA with multiple comparisons testing ($p < 0.05$ considered significant) in our analysis of the bladder cell and rat bladder wall morphological data.

Results

Lactobacillus Predominates the Human Bladder Microbiome

16S rRNA gene sequencing was performed on bladder trigone tissue from 20 patients (n=6 with detectable microbiome) to characterize the local microbiota. Sequencing of the 6 samples (patient gateway 1–6, PG1-6) generated a total of 463,097 paired-end reads. After quality control and merging of the paired-end reads, 414,281 clean reads were obtained in total, with at least 56,950 clean reads generated for each sample and an average of 69,047 clean reads produced per sample (Figure 2A).

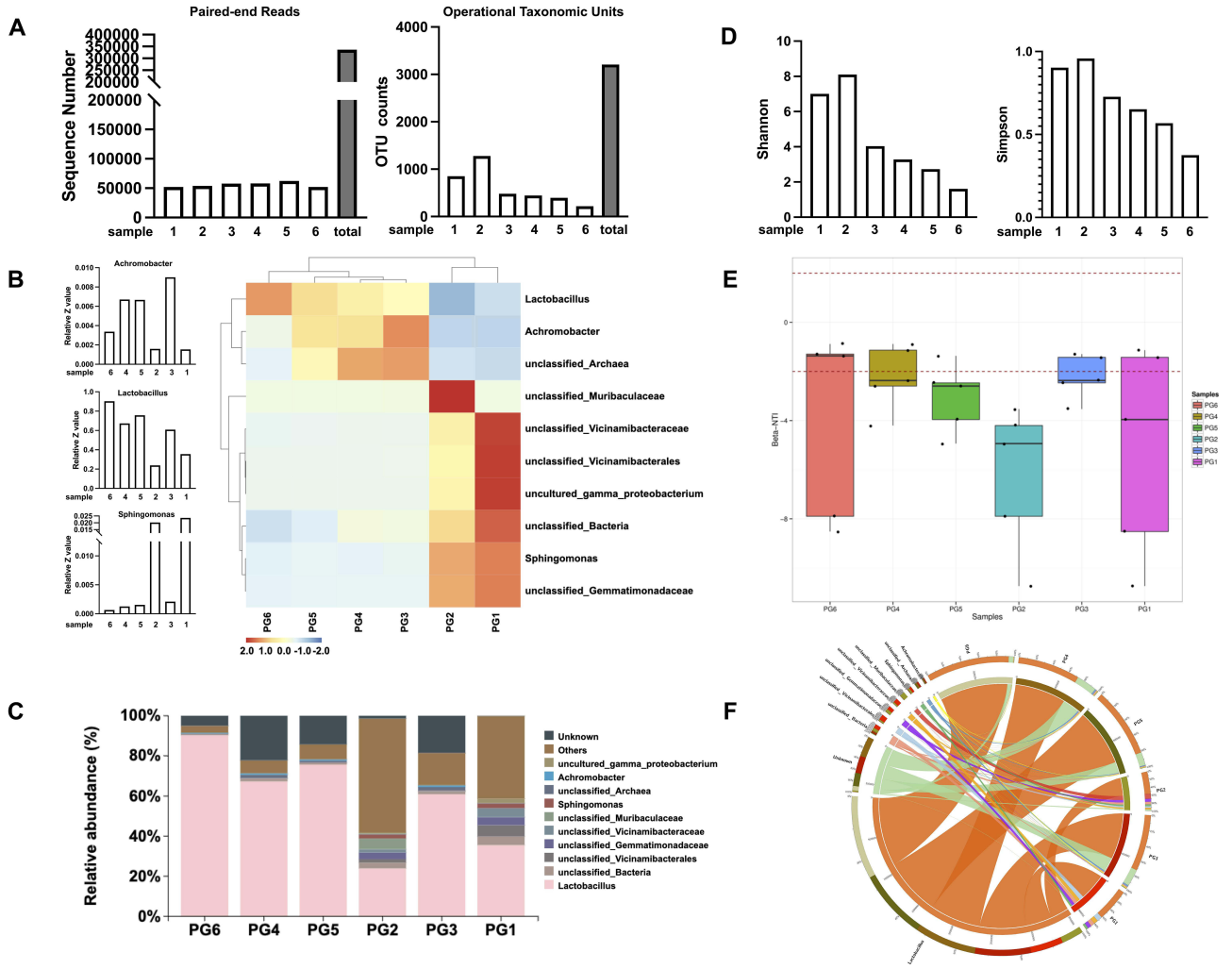

Figure 2 16S rRNA gene sequencing analysis to characterize the local microbiota. (**A**) High-throughput sequencing of 16S rRNA gene amplicons from bladder tissue biopsies of 6 patients, generating an average of 69,047 high-quality paired-end reads per sample. (**B**) Heatmap showing the top 10 most prevalent bacterial taxa across 6 patient samples (PG1-PG6). (**C**) Relative abundance analysis revealing Lactobacillus as the dominant bacterial genus, comprising over 60% of all bacterial sequences on average. (**D**) Microbial alpha diversity analysis using Shannon and Simpson ecological indices. (**E**) Beta diversity comparison between bladder tissue samples. (**F**) Circos plot illustrating relative abundance of bacterial genera. Samples are arranged clockwise around the circumference, with connecting ribbons to genera on the interior. Ribbon width corresponds to the percentage of sequences classified as that genus in each sample. This analysis provides insights into the bladder microbiome composition and diversity, highlighting the prevalence of Lactobacillus and the variability among patient samples.

Analysis of operational taxonomic units (OTUs) in the 16S rRNA sequencing data revealed varying numbers of OTUs across the six samples. Sample 1 contained 851 OTUs, sample 2 had 1279 OTUs, sample 3 had 482 OTUs, sample 4 had 444 OTUs, sample 5 had 396 OTUs, and sample 6 had 219 OTUs, for a total of 3209 OTUs detected across all samples. These results demonstrate that the microbial composition and diversity, as represented by unique OTUs, differed among the samples (Figure 2A). The total number of OTUs per sample may be indicative of overall species richness and evenness within that sample. Further analysis of the taxonomic classifications and relative abundances of the OTUs in each sample will provide insights into the distinctions in microbial community structure across the samples.[30]

The heatmap depicts the relative abundance profiles of the top 10 most abundant microbial taxa across the 6 samples as determined by 16S rRNA gene sequencing (Figure 2B). Hierarchical clustering grouped samples based on similarity in their microbial compositions. The colormap illustrates the abundance of each microbial taxon within each sample, with blue representing low abundance and red depicting high abundance. Several taxa, including unclassified Gemmatimonadaceae, Sphingomonas, and unclassified Bacteria, were prevalent across multiple samples. In contrast, other taxa like unclassified Archaea and Lactobacillus exhibited more sample-specific distributions. Overall, the heatmap

provides a visualization of the differences and similarities in microbial community structure across the samples, with clustering patterns indicating PG1/PG2 and PG3/PG4 contained more closely related compositions, while PG5/PG6 were more distinct.

Analysis of the 16S rRNA sequencing data revealed that Lactobacillus was the most highly abundant bacterial genus across the six bladder tissue samples, comprising an average of over 60% of total bacterial sequences. Specifically, Lactobacillus represented 90.299%, 67.31%, 75.67%, 23.91%, 60.91%, and 35.52% of the microbiota in samples PG6, PG4, PG5, PG2, PG3, and PG1, respectively (Figure 2C). The predominance of Lactobacillus suggests this bacterial genus may play important functional or ecological roles within the bladder tissue microbiome of the samples analysed.

Alpha diversity analysis (Shannon and Simpson) of the 16S rRNA gene sequencing data from six bladder tissue samples revealed varying levels of microbial diversity. The Simpson diversity index,[31] which measures community evenness, ranged from 0.3752 in sample 6 to 0.958 in sample PG2 (Figure 2D). Meanwhile, the Shannon diversity index,[31] which accounts for both richness and evenness, varied between 1.6095 in sample 6 and 8.1063 in sample PG2. The wide range of alpha diversity values indicates heterogeneity in the microbial diversity and composition among the tested bladder tissue samples (Figure 2D). Samples PG2 and PG3 exhibited higher diversity based on the alpha indices, suggesting more complex community structures. In contrast, samples PG5 and PG6 showed lower alpha diversity, implying relatively simpler or less even microbiota. Overall, these results demonstrate measurable differences in bacterial diversity across the bladder tissue samples, providing evidence that they represent suitable models for investigating the resident microbiota of the urinary system.

Beta diversity analysis using beta-nearest taxon index (β-NTI) revealed differences in community assembly processes across the six bladder tissue samples profiled by 16S sequencing.[32] The β-NTI values for samples PG6, PG4, PG3, and PG1 fell inside the −2 to 2 range, indicating their bacterial compositions were more influenced by random factors. In contrast, samples PG5 and PG2 exhibited β-NTI values are outside the −2 to 2 range, which means these cases have chances of being influenced by acquisition of bacteria from the environment rather than just ecological drift. These findings demonstrate heterogeneity in the ecological drivers of microbiota composition among the bladder tissue samples (Figure 2E).

The circos plot illustrates the relative abundances of bacterial taxa in each sample, with the six samples depicted on the right side of the circle and bacterial genera shown on the left. Connecting ribbons represent the abundance of each genus within each sample. The widths of the ribbons correspond to the percentage of sequences classified as a given genus in a particular sample. Orange ribbons predominate, representing the high relative abundance of Lactobacillus across samples (Figure 2F). This visualization demonstrates the compositional dominance of Lactobacillus, comprising over 50% of the microbiota on average, though its proportional representation varied among individual samples. Altogether, the circos plot provides an intuitive illustration of the taxonomic structure of the bladder tissue microbiome.

Lactobacillus Being a Benign Commensal Genus in the Bladder Niche

Functional profiling of the bladder tissue microbiome using BugBase predicted predominantly beneficial roles for Lactobacillus populations based on genomic content (Figure 3A). The phenotyping analysis characterized the bacterial taxa according to oxygen utilization, potential pathogenesis, and other traits.[33] Lactobacillus species were categorized as anaerobic, gram-positive, biofilm formers that lack mobile elements and are not typically pathogenic. This suggests the bladder-associated Lactobacillus communities have genomic features adapted to a benign commensal lifestyle rather than virulence. Given the high proportional abundances of Lactobacillus observed, these results imply this genus is suitably adapted for bladder colonization and likely plays a benign functional role in situ through anaerobic metabolism and biofilm formation without exerting harm.

Functional annotation of the 16S rRNA sequences using FAPROTAX predicted that the Lactobacillus populations in the bladder tissue microbiome were dominated by chemoheterotroph and fermentation pathways. The FAPROTAX phenotyping analysis categorized the bacterial taxa based on literature-curated information on cultivated microbes (Figure 3B).[34] Across the samples, Lactobacillus species comprised most sequences classified as chemoheterotrophs capable of utilizing organic compounds as energy and carbon sources. Lactobacillus sequences were also abundant among those annotated as fermenters that generate energy through substrate-level phosphorylation. These results suggest

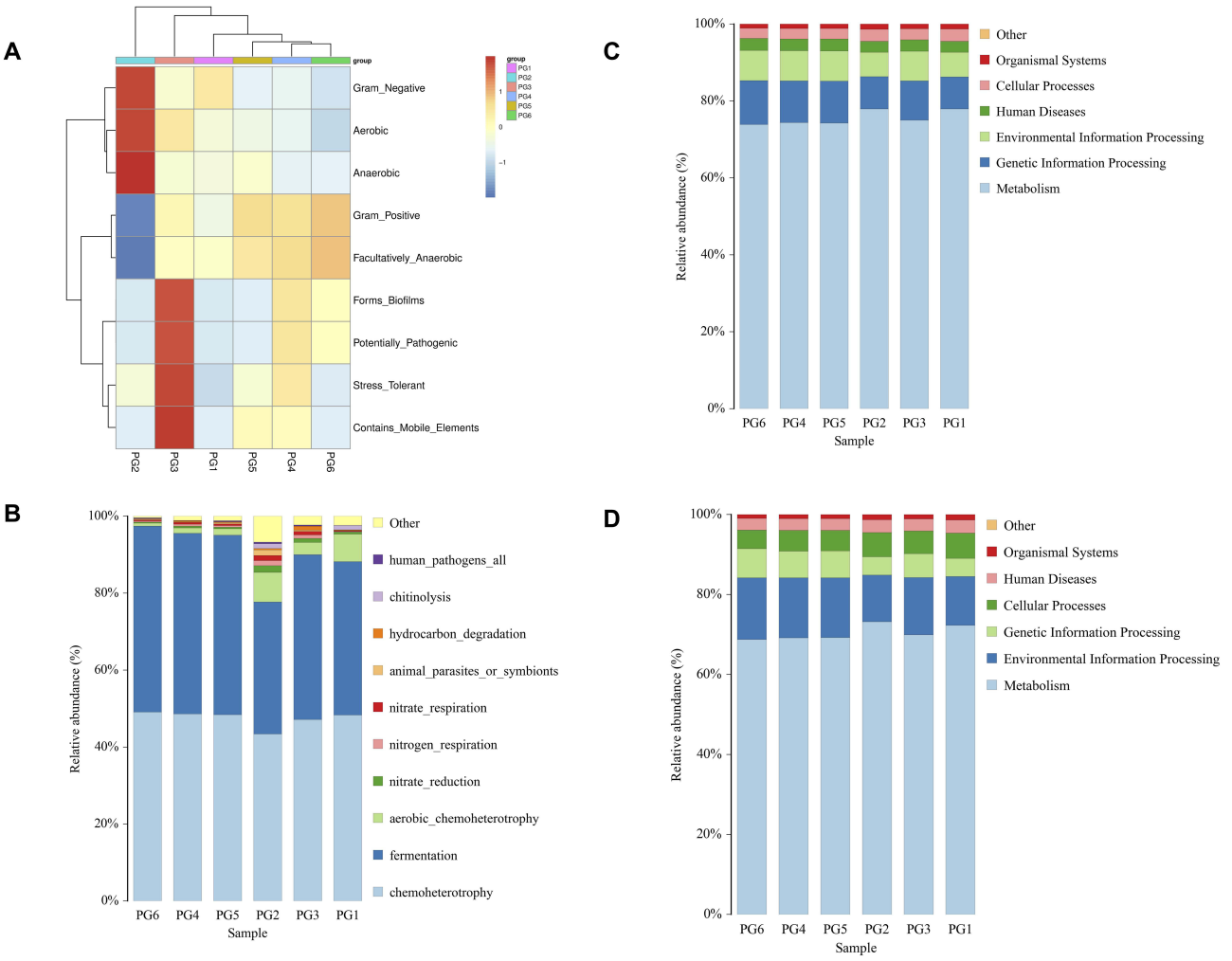

Figure 3 Lactobacillus being a benign commensal genus in the bladder niche. (**A**) In BugBase functional profiling, the high Lactobacillus abundance found implies these bacteria stably reside in the bladder, where they likely play functional metabolic and biofilm-forming roles without harm. (**B**) FAPROTAX functional annotation of sequences predicted the abundant Lactobacillus populations have genomes dominated by chemoheterotrophic and fermentative pathways. FAPROTAX categorized taxa based on cultivated microbes from literature. (**C**) PICRUSt2 analysis of samples reveals Lactobacillus plays a primarily beneficial functional role within the bladder microbiome. Lactobacillus metabolic activities focus heavily on essential processes-metabolism, genetic information processing, and environmental information processing. (**D**) Tax4Fun2 analysis highlights Lactobacillus as playing a pivotal beneficial role in the bladder microbiome, primarily driving essential metabolic functions along with environmental and genetic information processing.

the bladder-associated Lactobacillus communities have genomic content reflective of carbohydrate fermentation and chemoheterotrophic metabolisms. The predominance of these functional groups fits with Lactobacillus being a benign commensal genus in the bladder niche.

The results of the PICRUSt2 analysis conducted on six cases of bladder tissue samples reveal a noteworthy trend in the functional role of lactobacillus within the bladder microbiome (Figure 3C). Lactobacillus appears to primarily function as a benign bacterium, focusing its metabolic activities on various crucial processes.[35] Specifically, it is heavily involved in metabolism, genetic information processing, and environmental information processing. This suggests that Lactobacillus in bladder tissue primarily contributes to essential metabolic functions while also playing a role in the processing of genetic and environmental information. These findings underscore the potential beneficial impact of Lactobacillus in the bladder, as it contributes to the maintenance of important physiological processes and indicates a harmonious relationship between this genus and the host tissue.

The Tax4Fun2 analysis conducted on six cases of bladder tissue samples corroborates the findings from the PICRUSt2 analysis, highlighting the pivotal role of Lactobacillus as a benign bacterium within the bladder microbiome (Figure 3D).[36] Lactobacillus is shown to primarily engage in essential metabolic functions, as well as environmental and

genetic information processing. Specifically, the top three functions associated with Lactobacillus in bladder tissue include metabolism, environmental information processing, and genetic information processing. This consistency in results between Tax4Fun2 and PICRUSt2 analyses underscores the robustness of the findings. It reaffirms that Lactobacillus serves as a crucial contributor to maintaining bladder health by participating in key metabolic processes and facilitating the processing of genetic and environmental information.

LPS Demonstrate Enhanced Bladder Retention and Negligible Cytotoxicity in vitro

To determine the effects of PDA nanoparticles on Lactobacillus proliferation, relative growth rates were examined by optical density at 600 nm following incubation with 0.1, 0.5, and 2 mg/mL PDA for 1 hour. PDA exhibited negligible inhibitory activity against Lactobacillus across the tested concentrations. At the highest concentration of 2 mg/mL, PDA did not inhibit Lactobacillus proliferation (Figure 4A).

Additionally, the impacts of solifenacin on Lactobacillus were evaluated by optical density after exposure to 62.5–1000 nM solifenacin. Proliferation was largely unaffected by solifenacin up to 500 nM. At the maximum concentration of 1000 nM, minor inhibitory effects were observed, but Lactobacillus growth was largely unhindered. These data suggest solifenacin is unlikely to substantially inhibit the growth of this beneficial bacterium at physiologically relevant concentrations. Therefore, solifenacin appears to have negligible detrimental interactions with Lactobacillus that could disrupt the bladder microbiome, further supporting its safety profile (Figure 4B).

Electron microscopy revealed PDA nanoparticle decoration of Lactobacillus under different coating conditions. Upon morphological examination, PDA nanoparticles exhibited an aggregation tendency, forming clusters composed of multiple nanoparticles. With 0.1 mg/mL PDA, Lactobacillus exhibited sparse nanoparticle clusters randomly distributed on the cell surface. Increasing the concentration to 0.5 mg/mL PDA led to a continuous electron-dense layer enveloping the entirety of Lactobacillus. At the highest concentration of 2 mg/mL PDA, robust membrane-like coatings up to thick surrounded the Lactobacillus (Figure 4C). The size distribution analysis reveals notable differences between PDA nanoparticles synthesized at varying precursor concentrations. At low concentrations (0.5 and 1 mg/mL), the nanoparticles exhibit larger average diameters of around 90–120 nm with broad, potentially bimodal distributions skewed towards larger particle sizes exceeding 160 nm. However, at the optimal concentration of 2 mg/mL, there is a distinct shift to a tighter, unimodal distribution centered on a lower mean particle diameter around 70 nm. This non-linear trend suggests that the diameter of PDA nanoparticles initially decreases with increasing concentration of dopamine precursor before rebounding with excess amounts (Figure 4D).

In vitro proliferation of Lactobacillus was not negatively impacted by co-incubation with polydopamine or solifenacin. Growth curve analyses over 72 hours showed Lactobacillus cultivated with 2 mg/mL polydopamine or 500 μM solifenacin exhibited similar multiplication rates compared to control Lactobacillus grown without additives, as quantified by optical density measurements at 600 nm at regular intervals (Figure 4E). Final Lactobacillus densities achieved after incubation were comparable across groups. Additionally, disk diffusion assays revealed polydopamine and solifenacin did not produce zones of inhibition in Lactobacillus lawns on agar, and instead polydopamine and solifenacin alone or in combination could enhance Lactobacillus monoclonal spot proliferation (Figure 4G).

Gram staining of bladder tissue sections showed increased numbers of stained gram-positive bacilli in samples from rats treated with Lactobacillus-PDA compared to uncoated controls. Quantitative analysis determined a higher density of retained bacteria with polydopamine modification. Gram staining shows the penetrability in the Lactobacillus-PDA group (Control vs Lactobacillus-PDA group equals mean ± SEM: 1.8 ± 0.83 vs 5.8 ± 1.92; p=0.0027, Unpaired *t*-test) was increased compared to control (Figure 4F and H). Together, these results demonstrate polydopamine can be used to generate surface coatings on lactobacillus, subsequently enhancing bladder tissue binding and retention in vivo. Further optimization of the nanoparticle coating process is warranted to maximize bacterial adhesion while minimizing cytotoxicity (Figure 4F).

H-E staining revealed that the bladder wall remained structurally intact, displaying no signs of damage or disruption following treatment with lactobacillus and polydopamine-coated lactobacillus (LAC-PDA). This observation corroborates the preservation of bladder tissue integrity, with no discernible harm induced by the administered agents (Figure 4F). Masson staining further substantiated these findings by demonstrating the absence of any distinctive

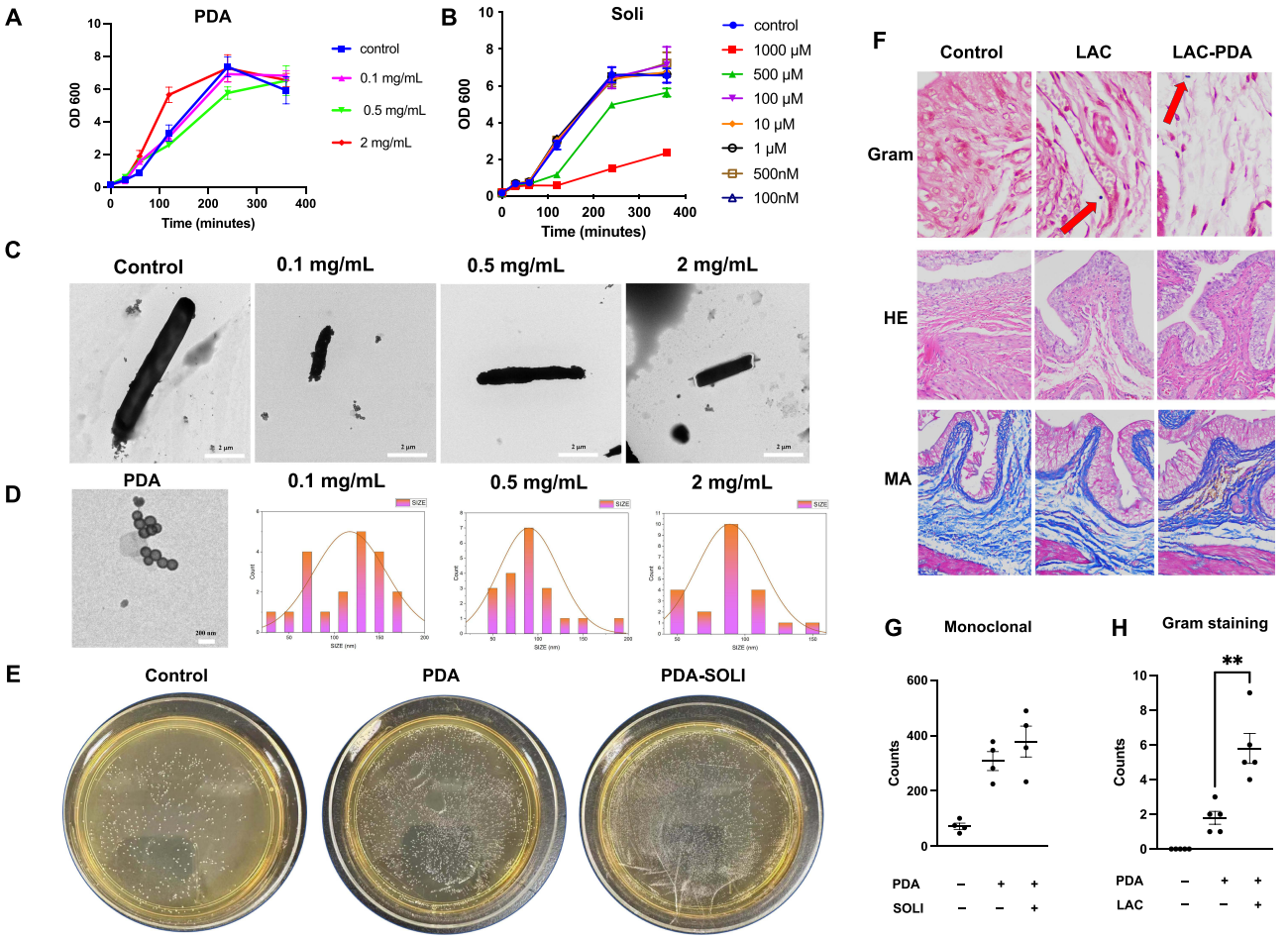

Figure 4 Encapsulation of solifenacin and PDA within Lactobacillus. (**A**) Lactobacillus proliferation after 1-hour exposure to 0.1–2 mg/mL PDA nanoparticles, showing negligible inhibition even at 2 mg/mL. (**B**) Solifenacin's impact on Lactobacillus growth at 62.5–1000 nM. (**C**) Electron microscopy revealing PDA nanoparticle decoration on Lactobacillus, with robust membrane-like coatings at 2 mg/mL PDA. (**D**) Size distribution of PDA nanoparticles at 0.1–2 mg/mL precursor concentrations, showing non-monotonic trend in mean diameter. (**E**) In vitro Lactobacillus proliferation unaffected by PDA or solifenacin co-incubation. (**F**) Gram staining of bladder tissue demonstrating increased gram-positive bacilli, with Lactobacillus (red arrow) penetrating the rat bladder wall. (**G**) Lactobacillus densities after incubation with/without additives; disk diffusion assays showed no inhibition zones. (**H**) Quantitative analysis revealing significantly higher bacterial retention with PDA modification (**p<0.01). These results illustrate PDA nanoparticles' and solifenacin's effects on Lactobacillus, highlighting enhanced bacterial retention and tissue penetration in the bladder microenvironment.

alterations in the bladder's histological layers and blood vessels within the bladder tissue that had been exposed to lactobacillus and LAC-PDA (Figure 4F and H). No evidence of fibrotic changes or abnormal collagen deposition was observed, indicating the maintenance of the tissue's normal architecture and vascular integrity.

LPS Penetrates 3D Bladder Cell Spheroids and Mitigates Drug-Induced Toxic Changes

HE-staining showed solifenacin treatment induced dysmorphic changes in 3D bladder cell spheroids, disrupting the distinct urothelial and smooth muscle layers evident in controls. However, these adverse effects on spheroid tissue architecture were mitigated when solifenacin was co-administered with the LPS (Figure 5A). Masson-staining confirmed LPS's protective effects, with preservation of the collagenous stromal layer compared to solifenacin alone. ImageJ analysis of spheroid borders revealed a smaller border area in LPS-treated spheroids compared to control and solifenacin-treated spheroids, as shown in Figure 5A. Additionally, quantification of spheroid diameters across treatment groups indicated that LPS exposure significantly reduced bladder cell spheroid diameter after 24 hours in culture when compared to untreated control spheroids. Spheroid diameter analysis shows the bladder cell spheroid formation in the LPS group (LPS vs Control equals mean ± SEM: 397.63 ± 70.39 vs 607.99 ±70.67; p=0.005, ordinary one-way ANOVA) was decreased compared to control (Figure 5B).

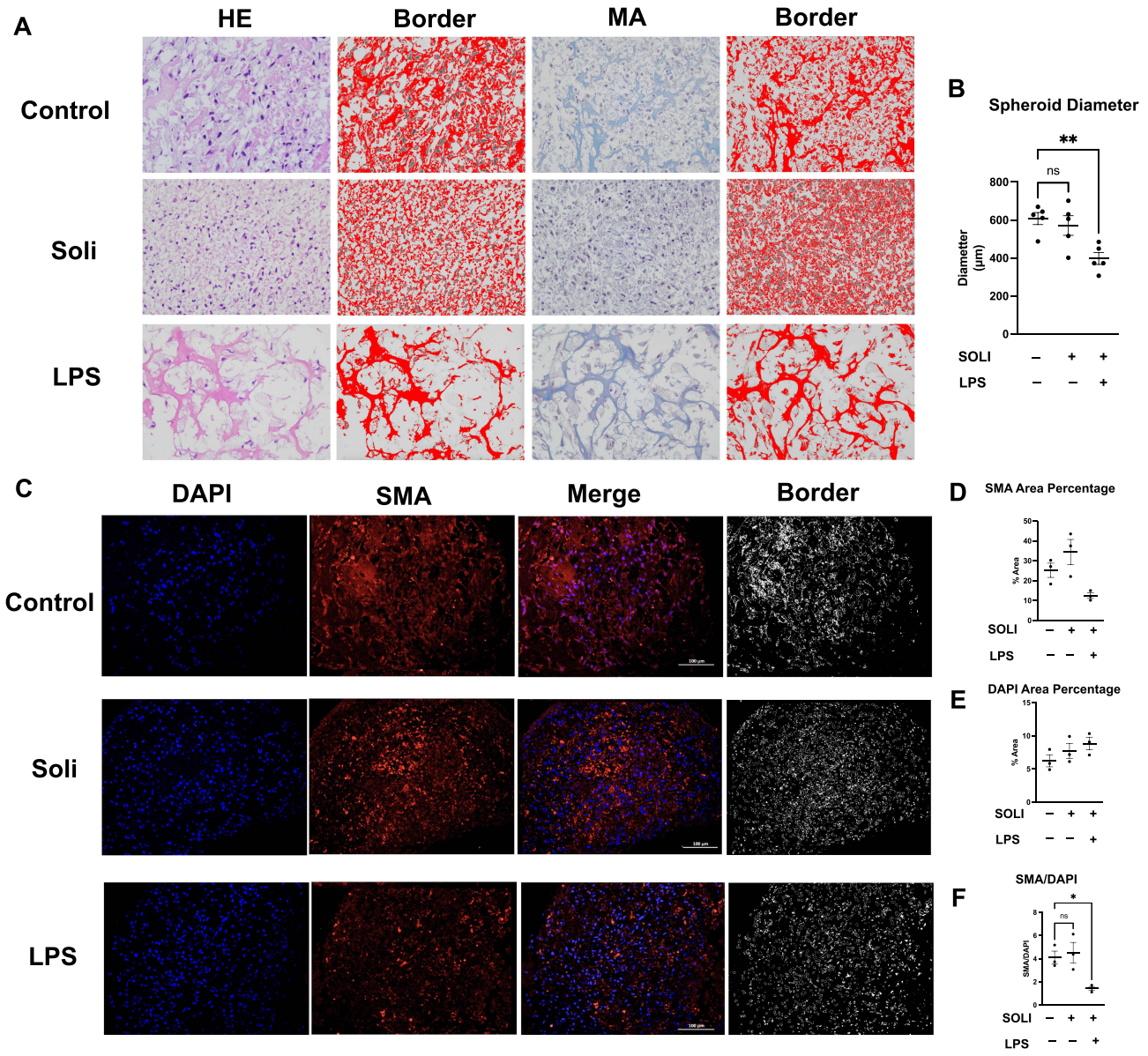

Figure 5 LPS for potential urological therapy in bladder smooth muscle cell spheroids. (**A** and **B**) HE staining showed solifenacin induced morphological changes in 3D bladder cell spheroids, disrupting distinct urothelial and smooth muscle layers seen in controls. However, co-administration with LPS mitigated these solifenacin-mediated adverse effects on spheroid architecture. LPS exposure significantly reduced spheroid diameter after 24 hours compared to untreated controls. Statistical significance (**p<0.01) demonstrated between groups. (**C**) IF staining revealed that LPS penetrated spheroid cores and increased α-smooth muscle actin (SMA) expression in inner smooth muscle cells, unlike solifenacin, which showed poor penetration and no protein level changes. (**D**–**F**) LPS treatment significantly decreased the ratio of SMA area to cell area compared to controls, altering spheroid morphology. While LPS did not change total cell numbers, it altered the distribution and structure of SMA-expressing cells within spheroids. Statistical significance (*p<0.05) was observed between groups.

IF staining studies revealed LPS could penetrate the core of spheroids and significantly decrease SMA expression in inner smooth muscle cells, suggesting direct modulatory effects on smooth muscle biology. In contrast, solifenacin monotherapy failed to effectively diffuse into the spheroid core and did not alter protein levels, indicating poor tissue penetration (Figure 5C).

Quantitative analysis of three independent IF staining revealed no significant differences in either SMA-positive or DAPI-stained areas between LPS-treated, solifenacin-treated, and control spheroids (Figure 5D and E). However, the ratio of SMA area to DAPI area was significantly decreased in LPS-treated spheroids compared to controls, suggesting that 24 hours of LPS exposure impacted spheroid formation and morphology. SMA/DAPI analysis shows the bladder cell spheroid formation in the LPS group (LPS vs Control equals mean ± SEM: 1.43 ± 0.29 vs 4.11 ± 0.94; p=0.0358, ordinary one-way ANOVA) was decreased compared to control. This ratio analysis indicates that while total cell numbers

(DAPI area) and SMA-positive cell proportions remained unchanged, LPS treatment altered the spatial distribution and structure of SMA-expressing cells within the spheroids (Figure 5F).

Therapeutic Effects of LPS in a Rat Overactive Bladder Model

OAB rat model was developed based on preliminary data and literature review to examine the effects of OAB severity. The protocol for establishing the OAB rat model is outlined in Figure 6A. Upon gross morphological examination, LPS treated bladders exhibited a visibly darker appearance compared to the other experimental groups, likely attributable to the black coloration of the LAC-PDA solution which was observable through the bladder wall upon abdominal incision (Figure 6B). In depth HE staining evaluations showed OAB rat bladder tissue sections treated with solifenacin nanoparticles exhibited intact, organized urothelium lining the bladder lumen. The urothelial cell layers appeared

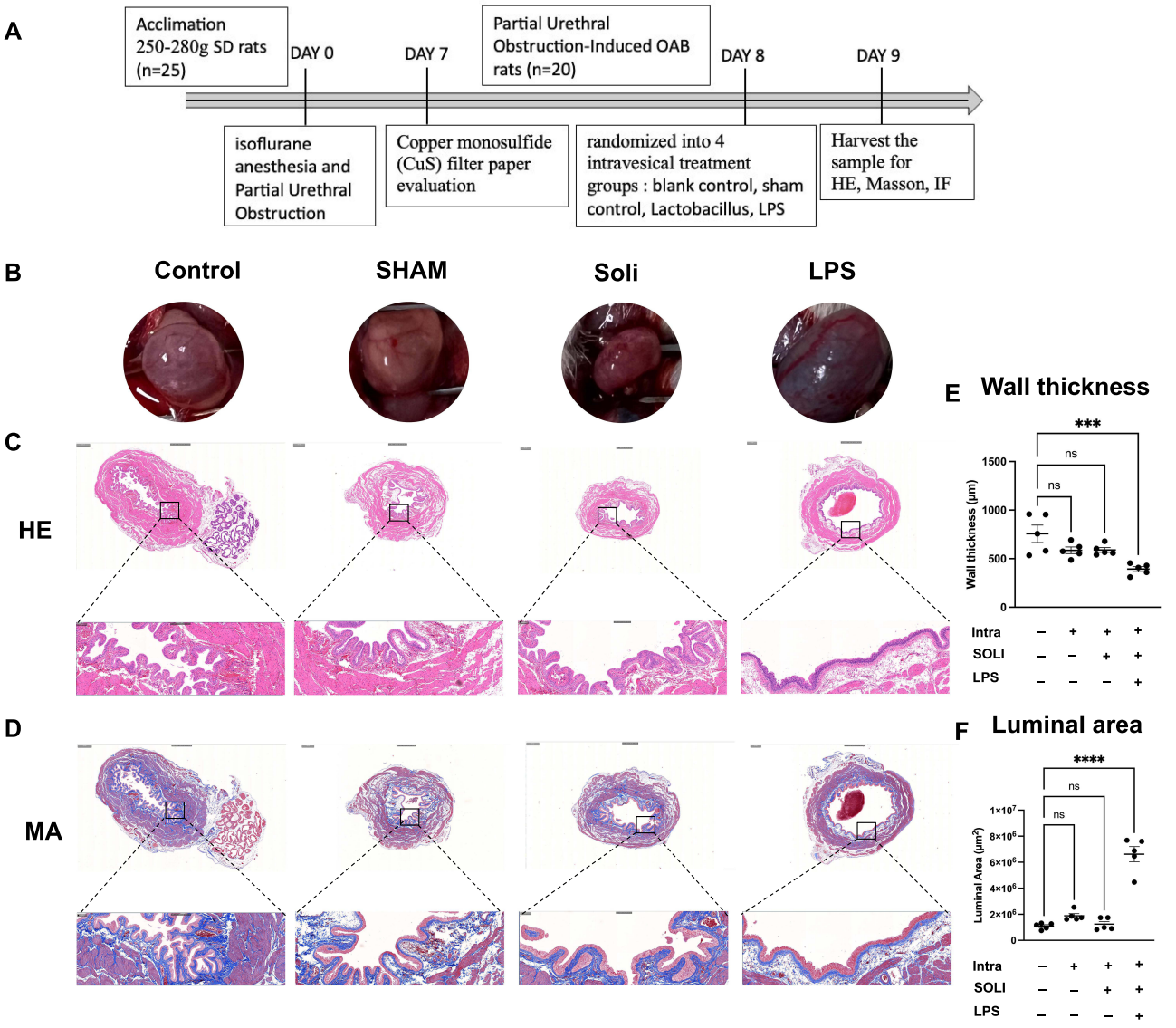

Figure 6 LPS facilitates the remodelling process of bladder in a rat OAB model. (**A**) Timeline for establishing the OAB rat model is outlined. (**B**) LPS-treated bladders exhibited darker appearance compared to other groups, attributable to dark color LAC-PDA solution visible through the bladder wall. (**C**) HE staining showed OAB rat bladder sections treated with solifenacin nanoparticles had intact, organized urothelium lining the lumen. Urothelial cell layers appeared compact with intact intracellular junctions and apical umbrella cells, similar to healthy controls. (**D**) Masson staining revealed sustained collagen distribution in solifenacin nanoparticle group bladder sections. (**E**) Quantitative analysis of HE/Masson-stained bladder sections revealed LPS administration significantly decreased bladder wall thickness compared to control and solifenacin groups. Statistical significance (***p<0.001) demonstrated between groups. (**F**) Analysis of Masson-stained bladder cross-sections showed LPS administration significantly increased luminal area compared to non-treated controls. Statistical significance (****p<0.0001) demonstrated between groups.

compact with intact intracellular junctions and apical asymmetric umbrella cells, similar to healthy controls. No desquamation, vacuolization, or necrosis was evident (Figure 6C). Smooth muscle bundles in the muscularis propria retained their interlacing architecture and normal morphology. Muscle fibers appeared tightly packed with centralized oval nuclei. No signs of myocyte degradation or inflammation were observed (Figure 6B). Quantitative image analysis of H-E/Masson-stained bladder sections from 5 rats per experimental group revealed that LPS (LPS vs Control equals mean ± SEM: 392.66 ± 57.22 μm vs 756.64 ± 200.22 μm; p=0.0004, ordinary one-way ANOVA) administration significantly decreased bladder wall thickness compared to control and solifenacin-treated rats (Figure 6E).

Likewise, Masson staining revealed sustained collagen distribution in bladder sections from solifenacin nanoparticle groups. Dense blue-stained collagen fibers were visible underlying the urothelium and surrounding smooth muscle bundles, comparable to control samples. No alteration in extracellular matrix composition or fibrosis was noted (Figure 6D). Bladder luminal areas were quantified in Masson-staining cross-sections from 5 rats per treatment group. ImageJ analysis using threshold measurement settings indicated LPS administration (LPS vs Control equals mean ± SEM: 6.619×10^6 μm^2 ± 1.307×10^6 vs 1.095×10^6 ± 2.39×10^6 μm^2; p<0.0001, ordinary one-way ANOVA) significantly increased luminal area compared to non-treated controls, as shown in Figure 6F.

IF imaging revealed nanoparticles loaded with solifenacin sustained expression of key smooth muscle filament proteins and SMA compared to bladders treated with LPS alone. Quantification of fluorescence intensity showed no significant differences in the levels of these contractile proteins versus healthy controls. In contrast, LPS stimulation substantially decreased filament protein expression (Figure 7A). Total smooth muscle cell numbers were unchanged

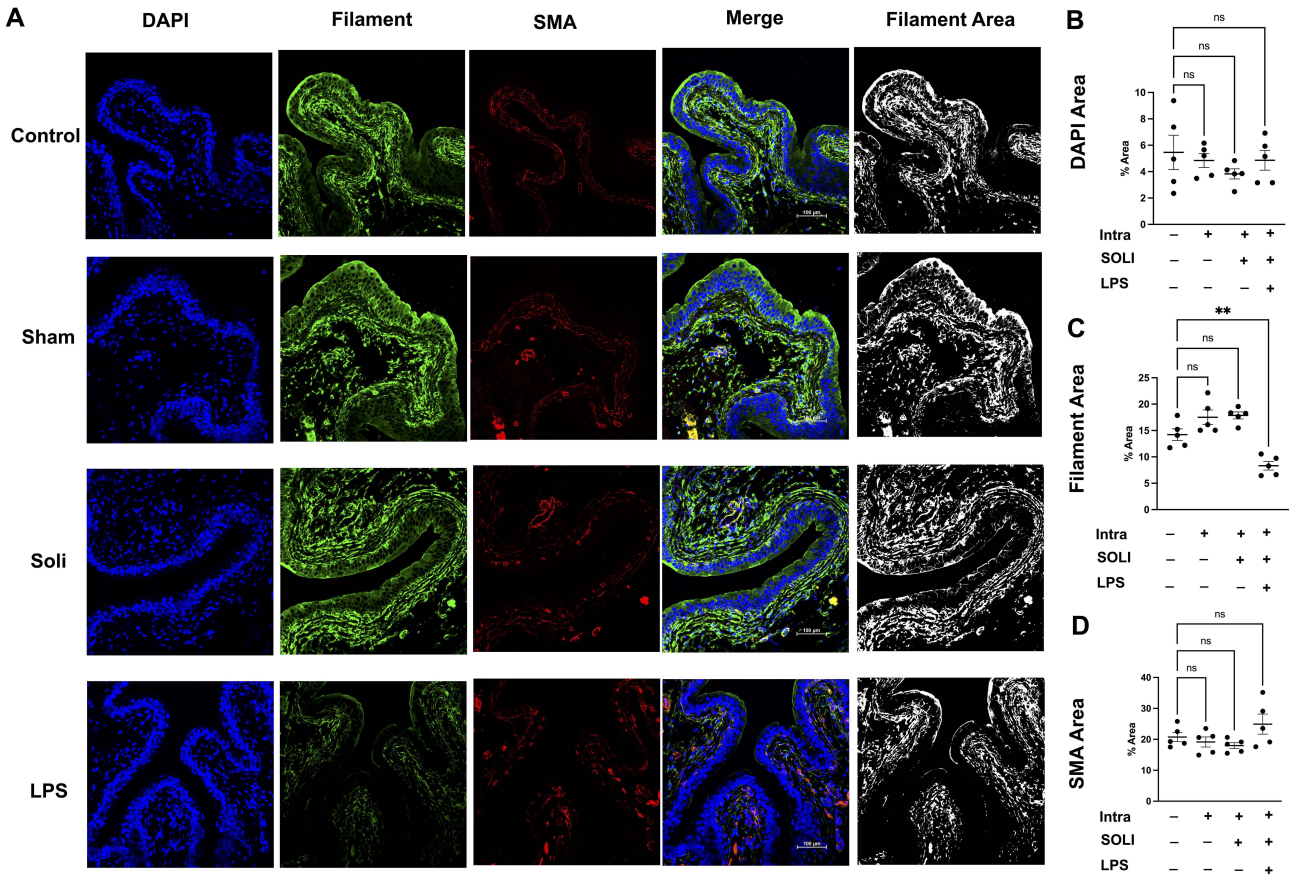

Figure 7 LPS decrease the expression and distribution of filament of bladder in a rat OAB model. (**A**) IF imaging showed nanoparticles with solifenacin sustained expression of key smooth muscle filament proteins and SMA compared to LPS alone. Quantification showed no significant differences in contractile protein levels versus healthy controls. In contrast, LPS stimulation substantially decreased filament protein expression. (**B**) DAPI area quantification revealed total smooth muscle cell numbers were unchanged between groups. (**C**) IF analysis showed no significant differences in proportions of SMA-positive area between groups. (**D**) Image analysis uncovered cytoskeletal filament morphology perturbations in LPS treated rats. Quantification of filament area in bladder sections showed a decrease with LPS compared to controls. Statistical significance (**p<0.01) demonstrated between groups.

according to the DAPI area (Figure 7B). Immunohistochemical analysis revealed no significant differences in proportions of SMA-positive area within bladder tissue between different groups (Figure 7C). However, fine resolution microscopy and ImageJ analysis uncovered perturbations in cytoskeletal filament morphology in LPS treated OAB rats. Quantification of filament area from in 5 individual bladder section samples showed a decrease in LPS rats bladder tissue compared to control group (LPS vs Control equals mean ± SEM: 8.33 ± 1.82 vs 14.22 ± 2.47; p=0.0026, ordinary one-way ANOVA) (Figure 7D).

Discussion

OAB severely impacts quality of life, though systemic anti-muscarinic medications demonstrate limited efficacy and compliance. Localized therapy represents a promising alternative but requires optimized carriers to penetrate the bladder wall and reach smooth muscle targets. An emerging concept is that commensal urinary microbiota modulates lower urinary tract health. 16S rRNA sequencing in this study verified Lactobacillus as the predominant genus inhabiting the bladder tissue without pathogenicity, motivating further investigation as a potential probiotic delivery vehicle.

Prior reports have sought to verify the presence of microbes in the urine of LUTS patients and elucidate associations between microbial community features and disease mechanisms.[11,15] However, these studies have predominantly focused on potentially pathogenic microorganisms while overlooking commensal microbes that may confer protective functions in the urinary system. In contrast, an emerging body of work has successfully delineated relationships between specific microbiota constituents and LUTS subtypes such as benign prostatic hyperplasia,[37] interstitial cystitis,[38] OAB,[39] and bladder outlet obstruction.[40] Nevertheless, no studies have yet investigated if the bladder wall serves as a niche harboring benign microbial community. Our study provides the first evidence that the bladder wall hosts a benign microbial community. Genomic analysis revealed Lactobacillus as the predominant commensal bacterium in bladder smooth muscle, coexisting without impairing organ function. This discovery suggests Lactobacillus's potential as a probiotic carrier for bladder treatments.

Unlike conventional therapeutic modalities, our current platform combines bionanomaterial techniques with polydopamine to achieve dual inhibition of muscarinic receptors via sustained solifenacin release alongside penetrating the bladder wall to stimulate durable suppression of smooth muscle filament formation and reorganization. The most important view has concentrated predominantly on urine-derived microbes, overlooking the possibility of benign bladder wall-associated microbiota. By harnessing this unique bladder niche, our bacteria-based nanomaterial approach overcomes the limitation of inadequate retention by promoting microbial vector integration and in situ embedding. This further enhances stable carriage and oriented release of pharmacologic cargo across the mucosa into underlying tissue.

In this study, we demonstrate proof-of-concept for an innovative microbe-assisted drug delivery (MADD) traversing the bladder permeability barrier to transport solifenacin, validating the clinical translational promise of harnessing endogenous microbe-mucosa interactions. Our adoption of Lactobacillus as a biocompatible vector refutes the classical sterile bladder notion, opening avenues for MADD and enabling sustained, localized antimuscarinic efficacy. In contrast to the daily oral administration of solifenacin,[9] our innovative LPS aims to provide a more targeted and potentially extended-duration treatment approach. Our preclinical rat studies involved administering solifenacin on day 8 to establish a robust evidence and collect comprehensive data on the system's efficacy and safety profile. Based on the animal data from our study, we anticipate that the clinical trial could involve a weekly treatment regimen. Furthermore, this pioneering approach surmounts the constraints of traditional pharmacotherapies through precision-targeted, sustained release of smooth muscle relaxants directly into bladder tissues. Our studies on Lactobacillus combined with polydopamine to deliver solifenacin overcome deficiencies of antimuscarinic drugs, serving as a paradigm for MADD.

LPS system enables facile infusion into the bladder wall by combining natural and synthetic materials through biologically inspired design and clinically relevant delivery methods. Bladder infusion serves as a clinically feasible approach to administer the LPS nanocomposite loaded with solifenacin, allowing diffusion across the urothelium and sustained retention within the bladder muscularis. PDA was selected owing to its approval for translational applications and ability to degrade into safe by-products, while also permitting loading of additional pharmacological agents to mitigate aberrant smooth muscle formation underlying LUTS.[41]

Our innovative approach leverages Lactobacillus, a natural bladder commensal, as a biocompatible vector to enhance tissue permeation, challenging traditional sterility concepts in drug delivery. The resulting LPS system, featuring a multifunctional PDA nanostructure with balanced degradation, enables sustained bladder wall diffusion and smooth muscle remodelling, potentially offering long-term relief for LUTS severity through flexible biomechanical remodelling and prolonged pharmacological efficacy.[42]

This biomimetic approach combining a bladder-derived microbe with advanced nanotechnology overrides prior constraints relying on inert nano-particulates lacking efficient retention or tissue integration.[43] Instead, the Lactobacillus vectors actively embed within the microenvironment, granting persistent localized drug release. This resonates with emerging host-microbiome paradigms recognizing that commensal organisms occupy specific niches enabling symbiotic functions. Co-opting this evolved crosstalk between bladder mucosa and microbiota surmounts permeability challenges that impede conventional pharmacological therapies.[44]

Taking together with multifaceted histological analyses, this study reveal co-delivery with LPS empowers solifenacin to permeate 3D bladder model, engage smooth muscle targets, and exert localized pharmacological actions, while simultaneously maintaining the morphological and structural integrity of the urothelium-smooth muscle microanatomy structure.

LPS demonstrates targeted bacteriotherapy as a potential new approach for OAB treatment. In human bladder cell spheroid and rat models, the system distributed throughout the bladder wall and enhanced outcomes versus systemic medication by increasing local drug concentrations while reducing systemic exposure. This overcomes limitations of current OAB therapies by leveraging endogenous microbiota for localized delivery of first-line medications. Modulating the bladder microbiome through engineered probiotics is an emerging opportunity. This platform could enable time-dependent dosing regimens more complex than a single infusion, customizing to patient needs. However, clinical translation requires further characterization of the human bladder microbiome in healthy and diseased states. Furthermore, rigorous clinical trials are essential to evaluate the safety, biodistribution, durability, and therapeutic efficacy of this approach in patients.[45] Optimization of nanoparticle design and bacterial strain selection can enhance drug loading, retention, and biocompatibility.[46] Overall, upon additional validation in human studies, this platform offers considerable promise for advancing OAB treatment through targeted and sustained local drug delivery.

Conclusion

In conclusion, we developed a novel lactobacillus-polydopamine nanoparticle platform that leverages endogenous bladder microbiota for targeted overactive bladder therapy. 16S rRNA sequencing verified Lactobacillus as the predominant bladder bacterium in humans. Coating Lactobacillus with polydopamine nanoparticles allowed antimuscarinic drug loading without impacting bacterial viability or function. In vitro and in vivo models demonstrated bladder tissue penetration and biocompatibility. This bacterionanotechnology system distributed throughout the bladder wall and facilitated localized drug delivery in a rat overactive bladder model, improving outcomes versus systemic medication.

Our findings provide novel concept for an engineered probiotic delivery system using synergistic integration of microbiota and nanotechnology. Further optimization of nanoparticle design and bacterial strain can enhance therapeutic efficacy. Additional preclinical evaluation is warranted along with clinical studies characterizing the human bladder microbiome in overactive bladder patients. With continued development, this innovative bacteriotherapy approach holds strong potential to overcome limitations of current medications through targeted local pharmacological therapy for bladder dysfunction.

Acknowledgment

The conceptualization of this research study and the initial preliminary work were selected for presentation at the American Chemical Society (ACS) Fall 2023 National Meeting & Exposition, San Francisco. The poster abstract, entitled “Polydopamine-Lactobacillus system for drug delivery to treat overactive bladder | Poster Board #3293”, was showed in the “Poster Abstracts - Division: [PMSE] Division of Polymeric Materials Science and Engineering” proceedings of the ACS SciMeeting on August 15, 2023. The digital poster can be accessed via the following URL: https://acs.digitellinc.com/p/s/polydopamine-lactobacillus-system-for-drug-delivery-to-treat-overactive-bladder-poster-board-3293-581793#:~:text=It%20could%20adhere%20to%20and,and%20reach%20the%20target%20cells.

Author Contributions

All authors made a significant contribution to the work reported, whether that is in the conception, study design, execution, acquisition of data, analysis and interpretation, or in all these areas; took part in drafting, revising or critically reviewing the article; gave final approval of the version to be published; have agreed on the journal to which the article has been submitted; and agree to be accountable for all aspects of the work.

Funding

This analysis and/or the underlying studies had been funded by the Li Huanying Foundation of Beijing (No. PYZ201503) and National Natural Science Foundation of China (No. 81900689). Neither funding sources were involved in study design, in collection, analysis and interpretation of data, in the writing of the report, or in the decision to submit the article for publication.

Disclosure

All authors declare that the research was conducted in the absence of any commercial or financial relationships that could be construed as a potential conflict of interest.

References

1. Palmer MH, Wu JM, Marquez CS, et al. "A secret club": focus groups about women's toileting behaviors. *BMC Womens Health*. 2019;19(1):44. doi:10.1186/s12905-019-0740-3
2. Chuang YC, Liu S-P, Lee K-S, et al. Prevalence of overactive bladder in China, Taiwan and South Korea: r esults from a cross-sectional, population-based study. *Low Urin Tract Symptoms*. 2019;11(1):48–55. doi:10.1111/luts.12193
3. Lightner DJ, Gomelsky A, Souter L, et al. Diagnosis and treatment of overactive bladder (Non-Neurogenic) in Adults: AUA/SUFU guideline amendment 2019. *J Urol*. 2019;202(3):558–563 doi:10.1097/JU.0000000000000309.
4. Nambiar AK, Arlandis S, Bø K, et al. European association of urology guidelines on the diagnosis and management of female non-neurogenic lower urinary tract symptoms. Part 1: diagnostics, overactive bladder, stress urinary incontinence, and mixed urinary incontinence. *Eur Urol*. 2022;82(1):49–59 doi:10.1016/j.eururo.2022.01.045.
5. Takahashi K, Tanaka T, Yoshizawa Y, et al. Lower urinary tract symptoms and functional ability in older adults: a community-based cross-sectional study. *BMJ Open*. 2022;12(4):e054530. doi:10.1136/bmjopen-2021-054530
6. Zhang AY, Xu X. Prevalence, burden, and treatment of lower urinary tract symptoms in men aged 50 and older: a systematic review of the literature. *SAGE Open Nurs*. 2018;4:2377960818811773. doi:10.1177/2377960818811773
7. Hughes FM, Odom MR, Cervantes A, et al. Why are some people with lower urinary tract symptoms (LUTS) Depressed? New evidence that peripheral inflammation in the bladder causes central inflammation and mood disorders. *Int J Mol Sci*. 2023;24(3):2821. doi:10.3390/ijms24032821
8. Steers WD. Pathophysiology of overactive bladder and urge urinary incontinence. *Rev Urol*. 2002;4(Suppl 4):S7–S18.
9. Chapple CR, Khullar V, Gabriel Z, et al. The effects of antimuscarinic treatments in overactive bladder: an update of a systematic review and meta-analysis. *Eur Urol*. 2008;54(3):543–562. doi:10.1016/j.eururo.2008.06.047
10. Zacche MM, Srikrishna S, Cardozo L. Novel targeted bladder drug-delivery systems: a review. *Res Rep Urol*. 2015;7:169–178. doi:10.2147/RRU.S56168
11. Yu SH, Jung SI. The potential role of urinary microbiome in benign prostate hyperplasia/lower urinary tract symptoms. *Diagnostics*. 2022;12(8):1 doi:10.3390/diagnostics12081862.
12. Brubaker L, Wolfe AJ. The new world of the urinary microbiota in women. *Am J Obstet Gynecol*. 2015;213(5):644–649. doi:10.1016/j.ajog.2015.05.032
13. Group NHW, Garges S, Giovanni M, et al. The NIH human microbiome project. *Genome Res*. 2009;19(12):2317–2323. doi:10.1101/gr.096651.109
14. Mostafaei H, Salehi-Pourmehr H, Rahnama'i MS, et al. Microbiome in Lower Urinary Tract Symptoms (LUTSs): mapping the state of the art with bibliometric analysis. *Life*. 2023;13(2). doi:10.3390/life13020552
15. Perez-Carrasco V, Soriano-Lerma A, Soriano M, et al. Urinary Microbiome: Yin and Yang of the Urinary Tract. *Front Cell Infect Microbiol*. 2021;11:617002. doi:10.3389/fcimb.2021.617002
16. Pearce MM, Hilt EE, Rosenfeld AB, et al. The female urinary microbiome: a comparison of women with and without urgency urinary incontinence. *mBio*. 2014;5(4):e01283–14. doi:10.1128/mBio.01283-14
17. Price TK, Hilt EE, Thomas-White K, et al. The urobiome of continent adult women: a cross-sectional study. *BJOG*. 2020;127(2):193–201. doi:10.1111/1471-0528.15920
18. Gottschick C, Deng Z-L, Vital M, et al. The urinary microbiota of men and women and its changes in women during bacterial vaginosis and antibiotic treatment. *Microbiome*. 2017;5(1):99. doi:10.1186/s40168-017-0305-3
19. Fouts DE, Pieper R, Szpakowski S, et al. Integrated next-generation sequencing of 16S rDNA and metaproteomics differentiate the healthy urine microbiome from asymptomatic bacteriuria in neuropathic bladder associated with spinal cord injury. *J Transl Med*. 2012;10:174. doi:10.1186/1479-5876-10-174
20. Wolfe AJ, Brubaker L. Urobiome updates: advances in urinary microbiome research. *Nat Rev Urol*. 2019;16(2):73–74. doi:10.1038/s41585-018-0127-5
21. Song CH, Kim YH, Naskar M, et al. Lactobacillus crispatus limits bladder uropathogenic E. coli infection by triggering a host type i interferon response. *Proc Natl Acad Sci U S A*. 2022;119(33):e2117904119. doi:10.1073/pnas.2117904119

22. Wu H, Wei M, Xu Y, et al. PDA-based drug delivery nanosystems: a potential approach for glioma treatment. *Int J Nanomed*. 2022;17:3751–3775. doi:10.2147/IJN.S378217
23. Loloi J, Babar M, Davies KP, et al. Nanotechnology as a tool to advance research and treatment of non-oncologic urogenital diseases. *Ther Adv Urol*. 2022;14:17562872221109023. doi:10.1177/17562872221109023
24. Jimenez-Jimenez C, Moreno VM, Vallet-Regi M. Bacteria-assisted transport of nanomaterials to improve drug delivery in cancer therapy. *Nanomaterials*. 2022;12(2):288. doi:10.3390/nano12020288
25. Esvaran M, Conway PL. Lactobacilli can attenuate inflammation in mouse macrophages exposed to polyethylene particles in vitro. *BMC Res Notes*. 2018;11(1):567. doi:10.1186/s13104-018-3676-z
26. Chapple CR, Cardozo L, Steers WD, et al. Solifenacin significantly improves all symptoms of overactive bladder syndrome. *Int J Clin Pract*. 2006;60(8):959–966. doi:10.1111/j.1742-1241.2006.01067.x
27. Bautista NBC, Dumancas GG, Ubas JG, et al. Quantification of lactobacillus reuteri proTectis in MRS broth using attenuated total reflectance–Fourier transform infrared (ATR-FTIR) spectroscopy and chemometrics. *J Agric Food Chem*. 2023;71:19101–19110. doi:10.1021/acs.jafc.3c04766
28. Li B, Yu Q, Wang R, et al. Inhibition of female and male human detrusor smooth muscle contraction by the rac inhibitors EHT1864 and NSC23766. *Front Pharmacol*. 2020;11:409 doi:10.3389/fphar.2020.00409.
29. Kim WH, Bae WJ, Park JW, et al. Development of an improved animal model of overactive bladder: transperineal ligation versus transperitoneal ligation in male rats. *World J Mens Health*. 2016;34(2):137–144. doi:10.5534/wjmh.2016.34.2.137
30. Chiarello M, McCauley M, Villéger S, et al. Ranking the biases: the choice of OTUs vs. ASVs in 16S rRNA amplicon data analysis has stronger effects on diversity measures than rarefaction and OTU identity threshold. *PLoS One*. 2022;17(2):e0264443. doi:10.1371/journal.pone.0264443
31. Willis AD, Martin BD. Estimating diversity in networked ecological communities. *Biostatistics*. 2022;23(1):207–222. doi:10.1093/biostatistics/kxaa015
32. Sinclair L, Osman OA, Bertilsson S, et al. Microbial community composition and diversity via 16S rRNA gene amplicons: evaluating the illumina platform. *PLoS One*. 2015;10(2):e0116955. doi:10.1371/journal.pone.0116955
33. Liu B, Lin W, Chen S, et al. Gut microbiota as an objective measurement for auxiliary diagnosis of insomnia disorder. *Front Microbiol*. 2019;10:1770. doi:10.3389/fmicb.2019.01770
34. Luo X, Gong Y, Xu F, et al. Soil horizons regulate bacterial community structure and functions in Dabie Mountain of the East China. *Sci Rep*. 2023;13(1):15866. doi:10.1038/s41598-023-42981-7
35. Carter KA, Fodor AA, Balkus JE, et al. Vaginal microbiome metagenome inference accuracy: differential measurement error according to community composition. *mSystems*. 2023;8(2):e0100322. doi:10.1128/msystems.01003-22
36. Wemheuer F, Taylor JA, Daniel R, et al. Tax4Fun2: prediction of habitat-specific functional profiles and functional redundancy based on 16S rRNA gene sequences. *Environmental Microbiome*. 2020;15(1):11. doi:10.1186/s40793-020-00358-7
37. Mariotti ACH, Heidrich V, Inoue LT, et al. Urinary microbiota is associated to clinicopathological features in benign prostatic hyperplasia. *Prostate*. 2023 doi:10.1002/pros.24649.
38. Zheng Z, Hu J, Li W, et al. Integrated microbiome and metabolome analysis reveals novel urinary microenvironmental signatures in interstitial cystitis/bladder pain syndrome patients. *J Transl Med*. 2023;21(1):266. doi:10.1186/s12967-023-04115-5
39. Peyronnet B, Mironska E, Chapple C, et al. A comprehensive review of overactive bladder pathophysiology: on the way to tailored treatment. *Eur Urol*. 2019;75(6):988–1000. doi:10.1016/j.eururo.2019.02.038
40. Antunes-Lopes T, Cruz F. Urinary biomarkers in overactive bladder: revisiting the evidence in 2019. *Eur Urol Focus*. 2019;5(3):329–336. doi:10.1016/j.euf.2019.06.006
41. Ji F, Sun H, Qin Z, et al. Engineering polyzwitterion and polydopamine decorated doxorubicin-loaded mesoporous silica nanoparticles as a pH-sensitive drug delivery. *Polymers*. 2018;10(3):326. doi:10.3390/polym10030326
42. Acter S, Moreau M, Ivkov R, et al. Polydopamine nanomaterials for overcoming current challenges in cancer treatment. *Nanomaterials*. 2023;13(10):1656. doi:10.3390/nano13101656
43. Jayasimha S. Nanotechnology in Urology. *Indian J Urol*. 2017;33(1):13–18. doi:10.4103/0970-1591.194780
44. Choi HW, Lee KW, Kim YH. Microbiome in urological diseases: axis crosstalk and bladder disorders. *Investig Clin Urol*. 2023;64(2):126–139. doi:10.4111/icu.20220357
45. Neugent ML, Hulyalkar NV, Nguyen VH, et al. Advances in understanding the human urinary microbiome and its potential role in urinary tract infection. *mBio*. 2020;11(2). doi:10.1128/mBio.00218-20
46. Jia L, Zhang P, Sun H, et al. Optimization of nanoparticles for smart drug delivery: a review. *Nanomaterials*. 2021;11(11):2790. doi:10.3390/nano11112790